DISTRIBUTION OF HENLE'S LOOPS MAY ENHANCE URINE CONCENTRATING CAPABILITY

H. E. LAYTON
Department of Mathematics, Duke University, Durham, North Carolina 27706

ABSTRACT A simple mathematical model that was developed by Charles S. Peskin (unpublished manuscript) for a single nephron is introduced and then extended to reflect the decreasing loop of Henle population as a function of increasing medullary depth. In the model, if all the loops turn at the same depth, the concentrating capability is limited by a factor of e over plasma osmolality. However, a decreasing loop population causes a multiplier effect that greatly enhances the concentrating capability. Using the loop distribution of the rat, the model produces a sigmoidal osmolality profile similar to the profiles found in tissue-slice studies of rat kidneys. These model calculations suggest that the decreasing nephron population found in vivo may be an important factor in the concentrating mechanism of the mammalian kidney.

INTRODUCTION

In the last forty-five years there have been many attempts to model the mammalian urine concentrating mechanism. Lists of relevant literature, along with some commentary, may be found elsewhere (Jacquez et al., 1976; Jamison and Kriz, 1982; Marsh, 1983). In recent years mathematical investigation of the concentrating mechanism has tended more toward detailed, large-scale simulation (e.g., Foster et al., 1976; Foster and Jacquez, 1978; Jacquez et al., 1976; Moore and Marsh, 1980; Moore et al., 1980; Stephenson et al., 1976) than toward schematic modeling (e.g., Marsh et al., 1967; Stephenson, 1973*a*, 1973*b*, 1976, 1981). Here, however, some new schematic models are developed. The goal is to construct the simplest reasonable model framework in which the effects of the loop of Henle distribution may be investigated.

Section I introduces a very simple mathematical model developed by Charles S. Peskin (unpublished manuscript). A single model nephron obeying a number of simplifying assumptions is able to bring urine osmolality up to only a factor of e (the Euler constant, $e \approx 2.7$) over plasma osmolality, regardless of the length of the loop of Henle or the type of kinetics specified for pumping NaCl from the ascending limb.

In section II a model for a discrete collection of nephrons, each similar to the single nephron of section I, but with varying loop of Henle lengths, is considered. A two-stage model is found to have a concentrating limit of e^2.

In section III the model framework is extended to represent a continuously decreasing loop population as a function of increasing medullary depth. This formulation leads to a coupled system of integral equations. Numerical solutions have been obtained by computer calculations, assuming specified loop distributions and Michaelis-Menten kinetics for pumping NaCl from the ascending limbs. If data for the rat loop distribution are used, computed concentration profiles are similar to those reported from tissue slice studies. These model results strongly suggest that the decreasing loop of Henle population common to many mammals contributes to urinary hypertonicity.

I. SINGLE-NEPHRON MODEL

In this section Peskin's mathematical model for a single medullary nephron in the antidiuretic state is introduced. After Peskin, the following assumptions are made:

- A0 The system is in steady state.
- A1 The descending limb, collecting duct, and distal convoluted tubule are permeable to water but not to solutes.
- A2 The descending limb, collecting duct, and interstitium have equal osmolalities at each medullary level, via trans-tubular water movement.
- A3 The fluid in the distal convoluted tubule equilibrates to plasma osmolality by water reabsorption.
- A4 The ascending limb is not permeable to water.
- A5 NaCl is actively reabsorbed from the ascending limb only.
- A6 There is no axial movement of fluid or solute in the interstitium.
- A7 The solute supplied to the interstitium by the ascending limb extracts water from the descending limb and collecting duct according to the relation $C = J_{2s}/J_v$, where C is the local interstitial osmolality, J_{2s} is the local NaCl reabsorption from the ascending limb, and J_v is the local water

reabsorption from the descending limb and collecting duct. The reabsorbed water and NaCl are picked up by the peritubular capillaries.

Assumptions A1–A6 are convenient idealizations based on a large body of experimental evidence (for an extensive survey, see Jamison and Kriz, 1982). There is no attempt to include in these assumptions all of the phenomena that may contribute to the concentrating mechanism. For example, even though there is experimental evidence that in some species significant solute enters the descending limb through the tubular membranes, this model assumes that the descending limb equilibrates by water reabsorption only. Moreover it is assumed here that all of the descending limbs are functionally alike, even though there is evidence that the descending limbs of short-looped nephrons differ in permeability properties from the descending limbs of long-looped nephrons (Imai et al., 1984; Imai, 1984).

To avoid detailed modeling of the complicated in vivo interaction between the interstitium and the peritubular capillaries, Peskin proposed A7 as a reasonable approximation for schematic modeling. He assumed that the interstitial fluid is picked up by a process analogous to glomerular ultrafiltration, but in the reverse direction. The driving force for this reverse filtration is the oncotic force of the plasma proteins, which are present in elevated concentrations in the peritubular capillaries due to differential filtration in the glomerulous. In effect, Peskin assumed that the peritubular capillaries act as a sink for locally reabsorbed water and solute, and that there is no other interaction between the capillaries and the interstitium.

Symbol and index conventions are listed in the Glossary. The configuration of the single-nephron model is shown in Fig. 1. In this simple, schematic model osmolality is computed on the basis of the total number of osmotically active particles, and the fluid volume is taken to be equal to the water volume which contains the solutes.

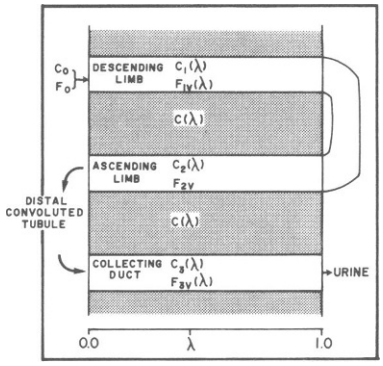

FIGURE 1 The configuration for the single-nephron model. By assumption A2, $C_1(\lambda) = C_3(\lambda) = C(\lambda)$; by A4, F_{2v} is constant.

GLOSSARY

Notation

Indices

i = 1 descending limbs(s)
2 ascending limb(s)
3 collecting duct(s)

k = v volume
s NaCl
u urea.

Symbols

α $C_{1u}(0)/C_{1s}(0)$; the ratio of urea to NaCl in the fluid entering the descending limbs

β TA/F_0

ϵ R_0/S_0; the fraction of S_0 that enters the collecting duct(s)

κ or λ the fractional axial distance along the medulla. $\lambda = 0$ at the cortico-medullary boundary; $\lambda = 1$ at the papillary tip

$\omega(\lambda)$ the fraction of loops of Henle reaching level λ

A the tubular area of an ascending limb having nondimensional length 1

B The maximum transport rate per unit of nondimensional length of a single ascending limb

$C(\lambda)$ the interstitial osmolality; in this model $C(\lambda)$ is also the osmolality in the descending limb(s) and in the collecting duct(s)

$C_i(\lambda)$ $C_{is}(\lambda) + C_{iu}(\lambda)$

$C_{ik}(\lambda)$ the osmolality at λ due to the solute k in the ith tubule

C_0 $C(0)$; the osmolality of fluid entering a descending limb at the cortico-medullary boundary; C_0 is approximately the osmolality of blood plasma.

$C_{2s}(\lambda, \kappa)$ the osmolality due to NaCl at level λ in the ascending limbs of loops that turned at level κ

$F_{ik}(\lambda)$ the flux at λ of the species k in the ith tubule

F_0 $F_{1v}(0)$; the volume flux entering a descending limb at the cortico-medullary boundary

$F_{2v}(\lambda, \kappa)$ the fluid flux at λ in the ascending limbs of loops that turned at level κ

$J_{ik}(\lambda)$ the rate of reabsorption at λ of the species k from the ith tubule

$J_{2s}(\lambda, \kappa)$ the rate of NaCl reabsorption at level λ from the ascending limbs of loops that turned at level κ

M the NaCl osmolality in an ascending limb when the transmural transport rate is at half maximum, i.e., the Michaelis constant

N_0 the number of loops of Henle

$R(\lambda, \kappa)$ the rate of NaCl transport per unit tubular area at level λ from a loop that turns at level κ

R_0 the solute flux entering the collecting duct(s)

S_0 $N_0C_0F_0$: the total solute flux entering the descending limb(s)

T a pump constant chosen so that TM is the maximum NaCl transport rate per unit tubular area of an ascending limb.

At each λ in the ith tubule, solute flux is given by $C_i(\lambda)F_{iv}(\lambda)$. Solute conservation in the descending limb and the collecting duct and assumption A1 imply that

$$C_1(\lambda)F_{1v}(\lambda) = S_0 \tag{1}$$

and

$$C_3(\lambda)F_{3v}(\lambda) = R_0, \tag{2}$$

where S_0 is the solute flux entering the descending limb at the cortico-medullary boundary and R_0 is the solute entering the collecting duct at the cortico-medullary boun-

dary. By the definitions of F_{1v} and F_{3v},

$$\frac{d}{d\lambda}[F_{1v}(\lambda) + F_{3v}(\lambda)] = -[J_{1v}(\lambda) + J_{3v}(\lambda)]. \quad (3)$$

By substituting Eqs. 1 and 2 in Eq. 3, and using A2 and A7, one obtains

$$\left(\frac{d}{d\lambda}C(\lambda)\right) \Big/ C(\lambda) = J_{2s}(\lambda)/(S_o + R_o). \quad (4)$$

By assumptions A1 and A5, and by solute conservation in the descending and ascending limbs,

$$R_o = S_o - \int_0^1 J_{2s}(\lambda)\, d\lambda. \quad (5)$$

Integrating Eq. 4 from 0 to 1 and using Eq. A3 and Eq. 5, one obtains

$$C(1)/C(0) = \exp(\tau/(2 - \tau)), \quad (6)$$

where τ is the fraction of solute flux that is reabsorbed from the ascending limb

$$\tau = \int_0^1 J_{2s}(\lambda)\, d\lambda / S_o. \quad (7)$$

τ is constrained to be less than or equal to 1, because, per unit time, more solute cannot be pumped from the ascending limb than is entering the descending limb. Note that τ does not depend on the explicit functional form of $J_{2s}(\lambda)$, but only on the rate of solute reabsorption from the whole length of the ascending limb.

Since $0 \le \tau \le 1$, one has $0 \le \tau/(2 - \tau) \le 1$, which implies that

$$1 \le C(1)/C_o \le e. \quad (8)$$

Thus under assumptions A0 through A7 there is a limit to the concentrating capability of this model nephron, and that limit is independent of the length of the loop of Henle and of the kinetics employed in the ascending limb. The same limit would apply to a collection of model nephrons all of the same length and arranged in parallel.

This model may be modified to reflect the loss of a solute, say urea, from the collecting duct. It is easy to show that the single nephron can still concentrate only up to a factor of e.

While there are some mammals with very low concentrating capability (e.g., the beaver, which can only concentrate up to about a factor of 2 [Schmidt-Nielsen and O'Dell, 1961]), the single-nephron model is an inadequate model for the general mammalian urine concentrating mechanism, because most mammals can concentrate well above a factor of e (e.g. man: 4; rat: 9; *Psammomys:* 16 [Schmidt-Nielsen and O'Dell, 1961]). This suggests that one or more of the assumptions of the model is faulty. Particularly suspect are assumption A1 (there may be solute addition to the ascending limb), assumption A7, and the use of a single-nephron model, which is equivalent to a model where all the nephrons are in parallel and have the same length. In many mammals the population of loops of Henle decreases dramatically as a function of medullary depth (see discussion in Jamison and Kriz, 1982). In the remainder of this report, the consequences of that structural characteristic are investigated, while assumptions A0–A7 are retained.

Geometrical features of renal architecture have been included in some previous models of nephron function. Sasaki and Suwa (1969) attempted to take into account the loop of Henle distribution in a schematic model of the inner medulla, but their assumptions for tubular permeability and transport properties differ markedly from those supported by recent experiments. Jacquez et al. (1976) and Foster et al. (1976) compensated for varying tubular diameters as a function of medullary depth, but did not study the effects of varying loop lengths. Moore and Marsh (1980) used a linear, but discrete, decrease in loop population in the inner medulla, but reached no conclusions on the importance of loop distributions, as it was not an objective of their study. Stephenson (1976, 1981) has developed schematic models with varying loop lengths; and in association with others, he has developed simulations with varying ratios of short to long loops (e.g., Mejia and Stephenson, 1984). Stephenson has suggested that the short nephrons are important in supplying enough urea to run the hypothesized passive inner medullary concentrating mechanism (1983), and he has hypothesized a cascade effect that enhances the passive mechanism through the varying solute concentrations in ascending limbs at a given level (1976). The analysis in the remainder of this article lends support to the importance of a cascade effect, especially for obtaining a high NaCl gradient in the inner medulla.

II: MULTINEPHRON MODEL WITH A DISCRETE LOOP DISTRIBUTION

This section and its sequel take into account the decreasing loop of Henle population found at increasing inner medullary depths in some mammals (e.g., rats). A fraction of the loops of Henle are assumed to reach each medullary level, but otherwise the assumptions of the preceeding single-nephron model are retained. A calculation without specific kinetics shows that a two-stage multinephron model can concentrate beyond a factor of e, thus demonstrating that the single-nephron model need not be dismissed out-of-hand as being unrealistic because of its limited concentrating capability. The intuitive idea that is here incorporated into a mathematical framework is that shorter loops preconcentrate the fluid in the descending limbs of longer loops, thus generating a cascade effect that enhances urinary hypertonicity.

In the multinephron model each individual nephron obeys assumptions A0, A1, and A3–A5. The nephrons

interact in a common interstitial space by collectively obeying assumptions A2, A6, and A7. A specified fraction of the loops reaches each medullary level. Each nephron has the same input of fluid and solute flux at the corticomedullary boundary, and each nephron carries its alloted solute flux into its ascending limb at the turn of the loop. NaCl is reabsorbed from each ascending limb, but, in general, the NaCl concentrations in ascending limbs at the same level λ will not be equal.

Let $\omega(\lambda)$ be the fraction of loops of Henle reaching level λ and suppose that $\omega(\lambda)$ is piecewise constant, i.e., let $\omega(\lambda) = \omega_i$ for $\lambda \in [\lambda_i, \lambda_{i+1}]$, where $0 = \lambda_0, \lambda_1, \ldots, \lambda_i, \ldots, \lambda_n = 1$ partition the interval $[0, 1]$. Assume that $\omega_0 = 1$ and that $0 < \omega_{i+1} < \omega_i < 1$ for $i > 0$, since the fraction of nephrons reaching successive levels is decreasing. A three-stage model is represented in Fig. 2.

Conservation of solute in the descending limbs requires that

$$C(\lambda)\, F_{1v}(\lambda) = \omega_i S_o, \qquad \lambda \in [\lambda_i, \lambda_{i+1}]. \tag{9}$$

Eq. 2 applies in this model unaltered, and Eq. 3 applies except at the discontinuities of ω. If Eqs. 9 and 2 are substituted into Eq. 3, and if assumptions A2 and A7 are used, then one obtains the differential equation

$$\left(\frac{d}{d\lambda} C(\lambda)\right) \Big/ C(\lambda) = J_{2s}(\lambda)/(\omega_i S_o + R_o), \in \lambda\,[\lambda_i, \lambda_{i+1}]. \tag{10}$$

Integrating from 0 to 1, one obtains

$$C(1)/C_0 = \exp\left(\sum_{i=0}^{n-1} \int_{\lambda_i}^{\lambda_{i+1}} \frac{J_{2s}(\kappa)/S_o}{\omega_i + \epsilon}\, d\kappa\right), \tag{11}$$

where $\epsilon = R_o/S_o$, with R_o given by Eq. 5.

Since in the steady state the rate of solute reabsorbed from the ascending limbs in the interval $[\lambda, 1]$ cannot exceed the rate at which solute reaches level λ in the descending limbs, solute conservation requires that

$$\int_\lambda^1 J_{2s}(\kappa)\, d\kappa \le \omega(\lambda) S_o. \tag{12}$$

Since only a finite amount of solute can pass through a unit area of membrane per unit time, it is necessary to require that

$$J_{2s}(\lambda) \le \omega(\lambda) N_o B, \tag{13}$$

where N_o is the total number of loops of Henle and B is the maximum transport rate per unit of nondimensional length of a single ascending limb.

For a two-stage model nephron,

$$C(1)/C_o = \exp\left(\int_0^{\lambda_1} \frac{J_{2s}(\kappa)/S_o}{1+\epsilon}\, d\kappa + \int_{\lambda_1}^1 \frac{J_{2s}(\kappa)/S_o}{\omega_1 + \epsilon}\, d\kappa\right). \tag{14}$$

Let $I_0 = \int_0^{\lambda_1} J_{2s}(\kappa)\, d\kappa$ and $I_1 = \int_{\lambda_1}^1 J_{2s}(\kappa)\, d\kappa$. By Eq. 12, $I_1 \le \omega_1 S_o$ and $I_0 \le S_o - I_1$. If $I_1 = \omega_1 S_o$ and $I_0 = S_o - I_1$, then $\epsilon = 0$ and

$$C(1)/C_o = \exp(2 - \omega_1) \tag{15}$$

so long as $\omega_1 > 0$. If $\omega_1 < 1$, then $C(1)/C_o > e$; and as ω_1 tends to 0, $C(1)/C_o$ tends to e^2.

Thus if there are a few long-looped nephrons and many more short-looped nephrons, and if most of the solute entering the short loops is pumped from their ascending limbs, and if most of the solute entering the long loops is pumped from their ascending limbs in the region $[\lambda_1, 1]$, then the short loops concentrate almost up to a factor of e, and the long loops concentrate almost up to another factor of e. (Eq. 13 will be satisfied if the loss of solute from the ascending limbs is sufficiently evenly distributed and if the dimensional lengths corresponding to $[0, \lambda_1]$ and $[\lambda_1, 1]$ are sufficiently large, since B increases linearly as the dimensional length increases.)

A similar argument for the n-stage model shows that $C(1)/C_o \le e^n$, with the limit e^n being achieved only if all available solute is pumped from the ascending limbs at each stage.

If significant solute remains in the luminal fluid of the collecting ducts, the concentrating capability of a multistage model is severely compromised by the damping effect of the water that accompanies the solute. However, one can show by further calculations that if some of the solute in the collecting ducts (e.g., urea) is allowed to escape into the interstitium, then the concentrating capability is not so severely compromised, because of the accompanying loss of water from the collecting ducts.

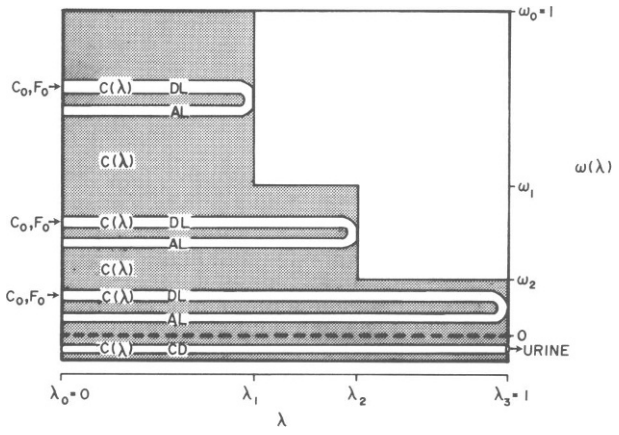

FIGURE 2 The configuration for a three-stage multinephron model. All of the loops of Henle reach level λ_1; a fraction ω_1 of the loops reach level λ_2; a fraction ω_2 of the loops reach level $\lambda_3 = 1$. DL = descending limb; AL = ascending limb; CD = collecting duct.

III: MULTINEPHRON MODEL WITH CONTINUOUS LOOP DISTRIBUTION

In this section, a continuous distribution of nephrons is considered; otherwise the assumptions of the discrete multinephron model of section II are retained. The precise

assumption for the turning of the loops is:

A8 In each interval $(\lambda, \lambda + \Delta\lambda)$, $[(\omega(\lambda) - \omega](\lambda + \Delta\lambda))N_0$ loops turn, carrying their alloted fraction of solute, $(\omega(\lambda) - \omega(\lambda + \Delta\lambda))S_0$, into the ascending limbs.

By conservation of solute in the descending limbs,

$$F_{1v}(\lambda) = \omega(\lambda)S_0/C(\lambda). \tag{16}$$

Differentiating Eq. 16 yields

$$-\frac{d}{d\lambda}F_{1v}(\lambda) = -\left(\frac{d}{d\lambda}\omega(\lambda)\right)S_0/C(\lambda) + (\omega(\lambda)S_0/C^2(\lambda))\frac{d}{d\lambda}C(\lambda), \tag{17}$$

where the first term on the right is the fluid that turns in the loops and the second term is $J_{1v}(\lambda)$. By essentially the same derivation used in section II to obtain Eq. 11, one obtains

$$C(\lambda)/C_0 = \exp\left(\int_0^\lambda \frac{J_{2s}(\kappa)/S_0}{\omega(\kappa) + \epsilon}\,d\kappa\right), \tag{18}$$

where $\epsilon = R_0/S_0$, with R_0 given by Eq. 5. As in section II, Eqs. 12 and 13 must be satisfied.

It is assumed that $J_{2s}(\lambda)$ depends on the NaCl concentrations in the ascending limbs, which depend on the kinetics of NaCl reabsorption and on the concentrations in the turns of the loops. For the loops that turn at λ, the osmolality of fluid is, of course, $C(\lambda)$, by assumption A2. Thus ultimately $J_{2s}(\lambda)$ depends on $C(\lambda)$. Since $C(\lambda)$ depends on $J_{2s}(\lambda)$ and ϵ, and ϵ depends on $J_{2s}(\lambda)$, one may obtain a coupled system of equations for the functions $C(\lambda)$ and $J_{2s}(\lambda)$ and the quantity ϵ.

In mammals with well-developed inner medullary regions, the ascending limbs of long-looped nephrons consist of two sections that differ morphologically, and, it is believed, functionally—the thick ascending limb in the outer medulla and the thin ascending limb in the inner medulla. It is generally accepted that NaCl is reabsorbed from the thick ascending limb by way of active Cl^- transport, with Na^+ following passively (Rocha and Kokko, 1973). The mechanism of NaCl reabsorption from the thin ascending limb is still in dispute, though many investigators favor the passive mechanism of Stephenson (1972) and Kokko and Rector (1972). In the heuristic model developed here, it is assumed for simplicity that NaCl reabsorption is by way of Michaelis-Menten kinetics along the entire length of the ascending limb.

If $J_{2s}(\lambda, \kappa)$ is the rate of NaCl reabsorption at λ from the loops that turn at κ, then the total rate of NaCl reabsorption at λ is given by

$$J_{2s}(\lambda) = \int_\lambda^1 J_{2s}(\lambda, \kappa)\,d\kappa. \tag{19}$$

$J_{2s}(\lambda, \kappa)\Delta\lambda\Delta\kappa$ is approximately the rate of NaCl reabsorption in the interval $[\lambda, \lambda + \Delta\lambda]$ from the loops which turn in the interval $[\kappa, \kappa + \Delta\kappa]$. If $R(\lambda, \kappa)$ is the rate of NaCl transport per unit tubular area at level λ from a loop which turns at level κ, then

$$J_{2s}(\lambda, \kappa)\Delta\lambda\Delta\kappa \approx R(\lambda, \kappa)A\Delta\lambda N_0(\omega(\kappa) - \omega(\kappa + \Delta\kappa)), \tag{20}$$

where A is the tubular area of an ascending limb of nondimensional length 1. Divide by $\Delta\lambda\Delta\kappa$ and let $\Delta\kappa \to 0$ to obtain

$$J_{2s}(\lambda, \kappa) = -R(\lambda, \kappa)AN_0\omega'(\kappa). \tag{21}$$

If Michaelis-Menten kinetics is specified for pumping NaCl from the ascending limbs, then

$$R(\lambda, \kappa) = TC_{2s}(\lambda, \kappa)/(1 + C_{2s}(\lambda, \kappa)/M) \tag{22}$$

for appropriate pump constants T and M.

$F_{2v}(\lambda, \kappa)C_{2s}(\lambda, \kappa)$ is the solute flux at λ in the ascending limbs of loops that turn at κ. By A4, $F_{2v}(\lambda, \kappa) = F_{2v}(\kappa, \kappa)$. By solute conservation,

$$J_{2s}(\lambda, \kappa) = \frac{\partial}{\partial\lambda}[F_{2v}(\kappa, \kappa)C_{2s}(\lambda, \kappa)]. \tag{23}$$

$F_{2v}(\lambda, \lambda)$ is given by the first term in Eq. 17. Insert Eq. 22 in Eq. 21 and equate the result with Eq. 23 to obtain the differential equation

$$\frac{\partial}{\partial\lambda}C_{2s}(\lambda, \kappa) = \beta(C(\kappa)/C_0)C_{2s}(\lambda, \kappa)/(1 + C_{2s}(\lambda, \kappa)/M), \tag{24}$$

where $\beta = TA/F_0$. Since the osmolality due to NaCl in the turns of the loops is the interstitial osmolality scaled by the fraction of solute that is NaCl, the boundary condition $C_{2s}(\kappa, \kappa) = C(\kappa)/(1 + \alpha)$ applies, where $\alpha = C_{1u}(0)/C_{1s}(0)$, the ratio of urea to NaCl entering the descending limbs. Eq. 24 has an implicit solution given by

$$\ln\left(\frac{C_{2s}(\lambda, \kappa)}{C(\kappa)/(1 + \alpha)}\right) + (C_{2s}(\lambda, \kappa) - C(\kappa)/(1 + \alpha))/M = \beta(C(\kappa)/C_0)(\lambda - \kappa). \tag{25}$$

Now using Eqs. 21, 22, and 19, the equation for $J_{2s}(\lambda)$ is obtained (Eq. 27 below) with $C_{2s}(\lambda, \kappa)$ solving Eq. 25. The complete set of equations is

$$C(\lambda)/C_0 = \exp\left(\int_0^\lambda \frac{J_{2s}(\kappa)/S_0}{\omega(\kappa) + \epsilon}\,d\kappa\right) \tag{26}$$

$$J_{2s}(\lambda)/S_0 = \int_\lambda^1 -\frac{\beta M}{C_0}\omega'(\kappa)\frac{C_{2s}(\lambda, \kappa)/M}{1 + C_{2s}(\lambda, \kappa)/M}\,d\kappa \tag{27}$$

$$\epsilon = 1 - \int_0^1 J_{2s}(\lambda)/S_0\,d\lambda. \tag{28}$$

It can be verified that Eqs. 12 and 13 are satisfied by $J_{2s}(\lambda)$ as it is given in Eq. 27. For this problem it is natural to specify ω, α, β, and M and then solve the system of integral equations for $C(\lambda)/C_0$, $J_{2s}(\lambda)/S_0$, and ϵ.

The existence of solutions to the integral equations is guaranteed by the Schauder principle. Uniqueness of solutions has been established only for the case of very small β. No evidence of nonuniqueness was observed in the numerical trials.

In the Appendix, the function ω has been estimated from experimental data for the loop of Henle distribution in rats:

$$\omega(\lambda) = \begin{cases} 1, & 0 \le \lambda \le 0.40 \text{ (outer medulla)} \\ \left(\dfrac{1-\lambda}{1-0.40}\right)^d, & 0.40 \le \lambda \le 1 \text{ (inner medulla)}, \end{cases} \quad (29)$$

where d ranges from about 2.1 to 2.8. The value of α is estimated from experimental data to be ~0.05 (Hai and Thomas, 1969). M is chosen to be C_0; and various values are assigned to β: 5.0, 7.5, and 10.

With these assumptions for ω, α, β, and M, Eqs. 26–28 were solved numerically. An iterative procedure was employed with the initial guess $C(\lambda)/C_0 = 1$. From this, $C_{2s}(\lambda, \kappa)/C_0$ was computed, then $J_{2s}(\lambda)/S_0$ and ϵ, and finally a new function $C(\lambda)/C_0$. The process was then repeated. For the class of parameters used in this study, the iterates of $C(\lambda)/C_0$ converged to agreement within 0.001 in approximately seven iterations.

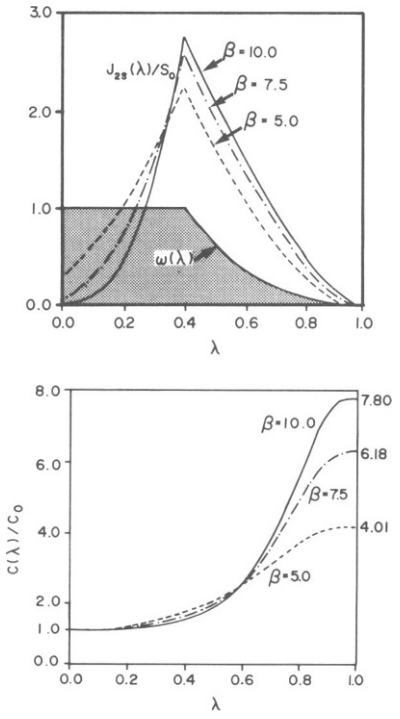

FIGURE 3 Computed profiles of $J_{2s}(\lambda)/S_0$ and $C(\lambda)/C_0$ using the rat loop distribution $\omega(\lambda)$ (Eq. 29 with $d = 2.5$). (*A*) $J_{2s}(\lambda)/S_0$ is the rate of NaCl reabsorption from the ascending limbs at λ scaled by S_0, the flux of solute into the descending limbs. (*B*) $C(\lambda)/C_0$ is the interstitial osmolality at level λ scaled by C_0, the plasma osmolality. For $\beta = 5.0$, 7.5, and 10, the resulting values of ϵ are 0.09, 0.06, and 0.05, respectively.

Some of the solution curves to Eqs. 26–28 are displayed in Fig. 3, where $\omega(\lambda)$, $J_{2s}(\lambda)/S_0$, and $C(\lambda)/C_0$ are plotted as profiles along the medullary axis. $J_{2s}(\lambda)$ is peaked near $\lambda = 0.40$ because more nephrons turn there and deposit solute than at any other level. The steep mid-portions of the curves $C(\lambda)/C_0$ result from the preconcentrating effect of shorter loops on longer ones. The leveling of the curves near $\lambda = 1$ (corresponding to the papillary tip) represents the damping effect of the urea-laden collecting ducts, which contain the predominant fluid flux there. This leveling would not be so pronounced if urea were permitted to escape from the collecting duct, because less water would then accompany the solute in the lower collecting duct. From the curves, it is clear that as β increases, the ratio $C(1)/C_0$ increases beyond the Euler constant e, and up to physiological values. Since $\beta = TA/F_0$, one can see that increasing the pump constant T, increasing the medullary length, or decreasing incoming single nephron fluid flux F_0 will all lead to increased $C(1)/C_0$.

The curves here obtained for $C(\lambda)/C_0$ are similar to those measured in rats in tissue-slice experiments by Hai and Thomas (1969). They obtained sigmoidal curves for tissue osmolality, tissue concentration of Na^+ and urea, and tissue content of Na^+ and urea. They also reported a very sharp increase in Na^+ tissue content near the boundary of the inner and outer medulla, perhaps corresponding to the peak of $J_{2s}(\lambda)$ in the model results.

ϵ represents the fraction of S_0 that is excreted in urine. Because of water and solute loss from the proximal convoluted tubule, S_0 is about a third of the filtered solute flux. About 0.01 of the filtered solute is excreted in vivo (Lassiter et al., 1961), so the in vivo value of ϵ is ~0.03. In the model, the calculated values of ϵ range from ~0.05 to 0.09 for values of the parameters M and β that give concentrations in the physiological range. The model's values for ϵ are higher than in vivo values probably because no solute is allowed to escape from the model's collecting duct.

Loop population profiles other than those for rats were investigated. It was found that if $\omega = 1$ for λ in the interval $[0, a]$, $0 < a < 1$, and ω decreases continuously to 0 at $\lambda = 1$, then, as $a \to 1$, the maximum concentrating capability of the multinephron model decreases to a factor of e over blood osmolality. This is expected, because in this limit the multinephron model should reduce to the model of the single nephron. Numerical results suggest that the loop population distribution in rats may be near optimal. For if the exponent d in Eq. 29 is chosen below or above physiological values (say $d = 1$ or $d = 3$), then the concentrating capability declines. Apparently decay that is too mild does not take optimal advantage of the cascade effect; and if the decay is too severe, then the presence of nonreabsorbable solute in the collecting duct along with its accompanying water moderates the concentrating capability near the papillary tip.

CONCLUDING REMARKS

While Peskin's single-nephron model can concentrate only up to a factor of e, the multinephron model exhibits a cascade effect that permits concentrations consistent with experimental measurements: solute reabsorbed from the ascending limbs of shorter-looped nephrons helps concentrate fluid in the descending limbs of longer-looped nephrons. This effect is particularly transparent in section II, where a distribution with many identical short loops and a few identical long loops is considered. The short loops are able to concentrate up to nearly a factor of e at the turns of their loops, because the damping effect of the few long loops is small. The long loops are then able to concentrate beyond e in the region where they extend beyond the short loops. In section III this idea is incorporated into a continuous process.

The passive concentrating mechanism suggested by Stephenson (1972) and Kokko and Rector (1972) cannot improve the concentrating capability of the single-nephron model, because, as already noted, the limit of e remains even if urea escapes from the collecting duct. However, a decreasing nephron population may help the passive mechanism in a multinephron model, since large amounts of the necessary urea will be available near the papillary tip. It is a natural next step to modify the mathematical framework developed here to study the passive mechanism.

Despite the simplifying assumptions and the limitations of the models presented here, it is believed that they make a strong case for the importance of the nephron distribution in the urine concentrating mechanism.

APPENDIX

The inner medullary nephron distribution for the rat given in Eq. 29 is based on the experimental measurements of Knepper et al. (1977) and Becker (1978). Knepper et al. measured the number of ascending limbs per unit cross-sectional area as a function of medullary depth; Becker measured the inner medullary cross-sectional area as a function of medullary depth. Using the product of the two measurements together, it is possible to estimate the in vivo population of loops of Henle as a function of medullary depth.

It is assumed that all nephrons have glomeruli in the cortex and that all loops of Henle reach at least as far as the inner-outer medullary boundary. The population density for the inner medulla is based on Fig. 4 in the article of Knepper et al. If the data represented there is plotted on log-log paper, the population density per unit area is found to be approximately proportional to $[(1 - \lambda)/(1 - 0.40)]^p$, where $p \approx 0.76$, 0.53, and 0.14 for rats R-2, R-4, R-3, respectively, and where the inner medulla extends from $\sim\lambda = 0.4$ to 1. The data of Becker suggest that the cross-sectional area of the inner medulla is proportional to $[(1 - \lambda)/(1 - 0.40)]^2$. Hence the inner medullay loop population is approximately proportional to $\omega(\lambda) = [(1 - \lambda)/(1 - 0.40)]^d$, where d ranges from $\sim$2.1 to 2.8.

The increasing loop population density reported by Knepper's group in the outer medulla as a function of increasing medullary depth is attributed by them to a significant decrease in medullary cross-section, rather than to a decrease in nephron population. Accordingly, it is assumed that $\omega = 1$ in the outer medulla.

The author gratefully acknowledges the helpful comments of Jacob J. Blum, Vincent W. Dennis, Leah Edelstein-Keshet, and Lazaro J. Mandel. Especial thanks are extended to Michael C. Reed for suggesting, sponsoring, and directing this research.

This work was supported in part by National Science Foundation grant DMS-8401590.

This work was originally published in abstract form (Nephron distribution enhances concentrating capability, 1985, *Fed. Proc.* 44:1913).

Received for publication 24 April 1985 and in final form 23 December 1985.

REFERENCES

Becker, B. 1978. Quantitative Beschreibung der Innenzone der Rattenniere. Inaugural-Dissertation, Universität Münster. Münster, West Germany.

Foster, D. M., and J. A. Jacquez. 1978. Comparison using central core model of renal medulla of the rabbit and rat. *Am. J. Physiol.* 234(5):F402–F414.

Foster, D., J. A. Jacquez, and E. Daniels. 1976. Solute concentration in the kidney—II. Input-output studies on a central core model. *Math. Biosci.* 32:337–360.

Hai, M. A., and S. Thomas. 1969. The time-course of changes in renal tissue composition during lysine vasopressin infusion in the rat. *Pfluegers Arch. Eur. J. Physiol.* 310:297–319.

Imai, M. 1984. Functional heterogeneity of the descending limbs of Henle's loop. II. Interspecies differences among rabbits, rats, and hamsters. *Pfluegers Arch. Eur. J. Physiol.* 402:393–401.

Imai, M., M. Hayashi, and M. Araki. 1984. Functional heterogeneity of the descending limbs of Henle's loop. I. Internephron heterogeneity in the hamster kidney. *Pfluegers Arch. Eur. J. Physiol.* 402:385–392.

Jacquez, J. A., D. Foster, and E. Daniels. 1976. Solute concentration in the kidney—I. A model of the renal medulla and its limit cases. *Math. Biosci.* 32:307–335.

Jamison, R., and W. Kriz. 1982. Urinary Concentrating Mechanism. Oxford University Press, New York. 340 pp.

Knepper, M. A., R. A. Danielson, G. M. Saidel, and R. S. Post. 1977. Quantitative analysis of renal medullary anatomy in rats and rabbits. *Kidney Int.* 12:313–323.

Kokko, J. P., and F. C. Rector, Jr. 1972. Countercurrent multiplication system without active transport in inner medulla. *Kidney Int.* 2:214–223.

Lassiter, W. E., C. W. Gottschalk, and M. Mylle. 1961. Micropuncture study of net transtubular movement of water and urea in nondiuretic mammalian kidney. *Am. J. Physiol.* 200(6):1139–1146.

Marsh, D. J. 1983. Computer simulation of renal counter-current systems. *Fed. Proc.* 42:2398–2404.

Marsh, D. J., R. B. Kelman, and H. C. Howard. 1967. The theory of urine formation in water diuresis with implications for antidiuresis. *Bull. Math. Biophys.* 29:67–89.

Mejia, R., and J. L. Stephenson. 1984. Solution for a multinephron, multisolute model of the mammalian kidney by Newton and continuation methods. *Math. Biosci.* 68:279–298.

Moore, L. C., and D. J. Marsh. 1980. How descending limb of Henle's loop permeability affects hypertonic urine formation. *Am. J. Physiol.* 239:F57–F71.

Moore, L. C., D. J. Marsh, and C. M. Martin. 1980. Loop of Henle during the water-to-antidiuresis transition in Brattleboro rats. *Am. J. Physiol.* 239:F72–F83.

Rocha, A. S., and J. P. Kokko. 1973. Sodium chloride and water transport in the medullary thick ascending limb of Henle: evidence for active chloride transport. *J. Clin. Invest.* 52:612–623.

Sasaki, Y., and N. Suwa. 1969. Functional model of inner medulla of rabbit kidney based on its structural principle. *Tohoku J. Exp. Med.* 98:33–36.

Schmidt-Nielsen, B., and R. O'Dell. 1961. Structure and concentrating mechanism in the mammalian kidney. *Am. J. Physiol.* 200:1119–1124.

Stephenson, J. L. 1972. Concentration of urine in a central core model of the renal counterflow system. *Kidney Int.* 2:85–94.

Stephenson, J. L. 1973*a*. Concentrating engines and the kidney: I. Central core model of the renal medulla. *Biophys. J.* 13:512–545.

Stephenson, J. L. 1973*b*. Concentrating engines and the kidney: II. Multisolute central core systems. *Biophys. J.* 13:546–567.

Stephenson, J. L. 1976. Concentrating engines and the kidney: III. Canonical mass balance equation for multinephron models of the renal medulla. *Biophys. J.* 16:1273–1286.

Stephenson, J. L. 1981. Concentrating engines and the kidney: IV. Mass balance in a single stage of a multistage model of the renal medulla. *Math. Biosci.* 55:265–278.

Stephenson, J. L. 1983. The renal concentrating mechanism: fundamental theoretical concepts. *Fed. Proc.* 42:2386–2391.

Stephenson, J. L., R. Mejia, and R. P. Tewarson. 1976. Model of solute and water movement in the kidney. *Proc. Natl. Acad. Sci. USA.* 73:252–256.